arXiv:0707.2462v1 [hep-ex] 17 Jul 2007

BELLE-CONF-0750
UCHEP-07-05

Search for B Meson Decays to ωK^{*0}

K. Abe,[10] I. Adachi,[10] H. Aihara,[52] K. Arinstein,[1] T. Aso,[56] V. Aulchenko,[1] T. Aushev,[22,16] T. Aziz,[48]
S. Bahinipati,[3] A. M. Bakich,[47] V. Balagura,[16] Y. Ban,[38] S. Banerjee,[48] E. Barberio,[25] A. Bay,[22] I. Bedny,[1]
K. Belous,[15] V. Bhardwaj,[37] U. Bitenc,[17] S. Blyth,[29] A. Bondar,[1] A. Bozek,[31] M. Bračko,[24,17] J. Brodzicka,[10]
T. E. Browder,[9] M.-C. Chang,[4] P. Chang,[30] Y. Chao,[30] A. Chen,[28] K.-F. Chen,[30] W. T. Chen,[28] B. G. Cheon,[8]
C.-C. Chiang,[30] R. Chistov,[16] I.-S. Cho,[58] S.-K. Choi,[7] Y. Choi,[46] Y. K. Choi,[46] S. Cole,[47] J. Dalseno,[25]
M. Danilov,[16] A. Das,[48] M. Dash,[57] J. Dragic,[10] A. Drutskoy,[3] S. Eidelman,[1] D. Epifanov,[1] S. Fratina,[17]
H. Fujii,[10] M. Fujikawa,[27] N. Gabyshev,[1] A. Garmash,[40] A. Go,[28] G. Gokhroo,[48] P. Goldenzweig,[3] B. Golob,[23,17]
M. Grosse Perdekamp,[12,41] H. Guler,[9] H. Ha,[19] J. Haba,[10] K. Hara,[26] T. Hara,[36] Y. Hasegawa,[45] N. C. Hastings,[52]
K. Hayasaka,[26] H. Hayashii,[27] M. Hazumi,[10] D. Heffernan,[36] T. Higuchi,[10] L. Hinz,[22] H. Hoedlmoser,[9] T. Hokuue,[26]
Y. Horii,[51] Y. Hoshi,[50] K. Hoshina,[55] S. Hou,[28] W.-S. Hou,[30] Y. B. Hsiung,[30] H. J. Hyun,[21] Y. Igarashi,[10]
T. Iijima,[26] K. Ikado,[26] K. Inami,[26] A. Ishikawa,[42] H. Ishino,[53] R. Itoh,[10] M. Iwabuchi,[6] M. Iwasaki,[52] Y. Iwasaki,[10]
C. Jacoby,[22] M. Jones,[9] N. J. Joshi,[48] M. Kaga,[26] D. H. Kah,[21] H. Kaji,[26] S. Kajiwara,[36] H. Kakuno,[52]
J. H. Kang,[58] P. Kapusta,[31] S. U. Kataoka,[27] N. Katayama,[10] H. Kawai,[2] T. Kawasaki,[33] A. Kibayashi,[10]
H. Kichimi,[10] H. J. Kim,[21] H. O. Kim,[46] J. H. Kim,[46] S. K. Kim,[44] Y. J. Kim,[6] K. Kinoshita,[3] S. Korpar,[24,17]
Y. Kozakai,[26] P. Križan,[23,17] P. Krokovny,[10] R. Kumar,[37] E. Kurihara,[2] A. Kusaka,[52] A. Kuzmin,[1] Y.-J. Kwon,[58]
J. S. Lange,[5] G. Leder,[14] J. Lee,[44] J. S. Lee,[46] M. J. Lee,[44] S. E. Lee,[44] T. Lesiak,[31] J. Li,[9] A. Limosani,[25]
S.-W. Lin,[30] Y. Liu,[6] D. Liventsev,[16] J. MacNaughton,[10] G. Majumder,[48] F. Mandl,[14] D. Marlow,[40]
T. Matsumura,[26] A. Matyja,[31] S. McOnie,[47] T. Medvedeva,[16] Y. Mikami,[51] W. Mitaroff,[14] K. Miyabayashi,[27]
H. Miyake,[36] H. Miyata,[33] Y. Miyazaki,[26] R. Mizuk,[16] G. R. Moloney,[25] T. Mori,[26] J. Mueller,[39] A. Murakami,[42]
T. Nagamine,[51] Y. Nagasaka,[11] Y. Nakahama,[52] I. Nakamura,[10] E. Nakano,[35] M. Nakao,[10] H. Nakayama,[52]
H. Nakazawa,[28] Z. Natkaniec,[31] K. Neichi,[50] S. Nishida,[10] K. Nishimura,[9] Y. Nishio,[26] I. Nishizawa,[54] O. Nitoh,[55]
S. Noguchi,[27] T. Nozaki,[10] A. Ogawa,[41] S. Ogawa,[49] T. Ohshima,[26] S. Okuno,[18] S. L. Olsen,[9] S. Ono,[53]
W. Ostrowicz,[31] H. Ozaki,[10] P. Pakhlov,[16] G. Pakhlova,[16] H. Palka,[31] C. W. Park,[46] H. Park,[21] K. S. Park,[46]
N. Parslow,[47] L. S. Peak,[47] M. Pernicka,[14] R. Pestotnik,[17] M. Peters,[9] L. E. Piilonen,[57] A. Poluektov,[1] J. Rorie,[9]
M. Rozanska,[31] H. Sahoo,[9] Y. Sakai,[10] H. Sakamoto,[20] H. Sakaue,[35] T. R. Sarangi,[6] N. Satoyama,[45] K. Sayeed,[3]
T. Schietinger,[22] O. Schneider,[22] P. Schönmeier,[51] J. Schümann,[10] C. Schwanda,[14] A. J. Schwartz,[3] R. Seidl,[12,41]
A. Sekiya,[27] K. Senyo,[26] M. E. Sevior,[25] L. Shang,[13] M. Shapkin,[15] C. P. Shen,[13] H. Shibuya,[49] S. Shinomiya,[36]
J.-G. Shiu,[30] B. Shwartz,[1] J. B. Singh,[37] A. Sokolov,[15] E. Solovieva,[16] A. Somov,[3] S. Stanič,[34] M. Starič,[17]
J. Stypula,[31] A. Sugiyama,[42] K. Sumisawa,[10] T. Sumiyoshi,[54] S. Suzuki,[42] S. Y. Suzuki,[10] O. Tajima,[10]
F. Takasaki,[10] K. Tamai,[10] N. Tamura,[33] M. Tanaka,[10] N. Taniguchi,[20] G. N. Taylor,[25] Y. Teramoto,[35]
I. Tikhomirov,[16] K. Trabelsi,[10] Y. F. Tse,[25] T. Tsuboyama,[10] K. Uchida,[9] Y. Uchida,[6] S. Uehara,[10] K. Ueno,[30]
T. Uglov,[16] Y. Unno,[8] S. Uno,[10] P. Urquijo,[25] Y. Ushiroda,[10] Y. Usov,[1] G. Varner,[9] K. E. Varvell,[47] K. Vervink,[22]
S. Villa,[22] A. Vinokurova,[1] C. C. Wang,[30] C. H. Wang,[29] J. Wang,[38] M.-Z. Wang,[30] P. Wang,[13] X. L. Wang,[13]
M. Watanabe,[33] Y. Watanabe,[18] R. Wedd,[25] J. Wicht,[22] L. Widhalm,[14] J. Wiechczynski,[31] E. Won,[19]
B. D. Yabsley,[47] A. Yamaguchi,[51] H. Yamamoto,[51] M. Yamaoka,[26] Y. Yamashita,[32] M. Yamauchi,[10] C. Z. Yuan,[13]
Y. Yusa,[57] C. C. Zhang,[13] L. M. Zhang,[43] Z. P. Zhang,[43] V. Zhilich,[1] V. Zhulanov,[1] A. Zupanc,[17] and N. Zwahlen[22]
(The Belle Collaboration)

[1]*Budker Institute of Nuclear Physics, Novosibirsk*
[2]*Chiba University, Chiba*
[3]*University of Cincinnati, Cincinnati, Ohio 45221*
[4]*Department of Physics, Fu Jen Catholic University, Taipei*
[5]*Justus-Liebig-Universität Gießen, Gießen*
[6]*The Graduate University for Advanced Studies, Hayama*
[7]*Gyeongsang National University, Chinju*
[8]*Hanyang University, Seoul*
[9]*University of Hawaii, Honolulu, Hawaii 96822*
[10]*High Energy Accelerator Research Organization (KEK), Tsukuba*
[11]*Hiroshima Institute of Technology, Hiroshima*

[12]*University of Illinois at Urbana-Champaign, Urbana, Illinois 61801*
[13]*Institute of High Energy Physics, Chinese Academy of Sciences, Beijing*
[14]*Institute of High Energy Physics, Vienna*
[15]*Institute of High Energy Physics, Protvino*
[16]*Institute for Theoretical and Experimental Physics, Moscow*
[17]*J. Stefan Institute, Ljubljana*
[18]*Kanagawa University, Yokohama*
[19]*Korea University, Seoul*
[20]*Kyoto University, Kyoto*
[21]*Kyungpook National University, Taegu*
[22]*Swiss Federal Institute of Technology of Lausanne, EPFL, Lausanne*
[23]*University of Ljubljana, Ljubljana*
[24]*University of Maribor, Maribor*
[25]*University of Melbourne, School of Physics, Victoria 3010*
[26]*Nagoya University, Nagoya*
[27]*Nara Women's University, Nara*
[28]*National Central University, Chung-li*
[29]*National United University, Miao Li*
[30]*Department of Physics, National Taiwan University, Taipei*
[31]*H. Niewodniczanski Institute of Nuclear Physics, Krakow*
[32]*Nippon Dental University, Niigata*
[33]*Niigata University, Niigata*
[34]*University of Nova Gorica, Nova Gorica*
[35]*Osaka City University, Osaka*
[36]*Osaka University, Osaka*
[37]*Panjab University, Chandigarh*
[38]*Peking University, Beijing*
[39]*University of Pittsburgh, Pittsburgh, Pennsylvania 15260*
[40]*Princeton University, Princeton, New Jersey 08544*
[41]*RIKEN BNL Research Center, Upton, New York 11973*
[42]*Saga University, Saga*
[43]*University of Science and Technology of China, Hefei*
[44]*Seoul National University, Seoul*
[45]*Shinshu University, Nagano*
[46]*Sungkyunkwan University, Suwon*
[47]*University of Sydney, Sydney, New South Wales*
[48]*Tata Institute of Fundamental Research, Mumbai*
[49]*Toho University, Funabashi*
[50]*Tohoku Gakuin University, Tagajo*
[51]*Tohoku University, Sendai*
[52]*Department of Physics, University of Tokyo, Tokyo*
[53]*Tokyo Institute of Technology, Tokyo*
[54]*Tokyo Metropolitan University, Tokyo*
[55]*Tokyo University of Agriculture and Technology, Tokyo*
[56]*Toyama National College of Maritime Technology, Toyama*
[57]*Virginia Polytechnic Institute and State University, Blacksburg, Virginia 24061*
[58]*Yonsei University, Seoul*

We report a search for the charmless vector-vector decay $B^0 \to \omega K^{*0}$ with 520×10^6 $B\overline{B}$ pairs collected with the Belle detector at the KEKB e^+e^- collider. We measure the branching fraction in units of 10^{-6}: $\mathcal{B}(B^0 \to \omega K^{*0}) = 1.2^{+0.9}_{-0.8} \pm 0.2$ (< 2.7), where the first error is statistical, the second systematic, and the upper limit is at the 90% confidence level.

Recently, $b \to sq\overline{q}$ penguin decays have received much attention in the literature. These decays proceed via an internal loop diagram and thus are potentially sensitive to new types of propagators and couplings. Such decays have sometimes yielded unexpected results, e.g., the $b \to su\overline{u}$ decay $B^0 \to K^+\pi^-$ exhibits substantial direct CP violation [1, 2], and the $b \to ss\overline{s}$ decay $B \to \phi K^*$ exhibits large transverse polarization [3, 4]. This latter observation implies that non-factorizable contributions to the decay amplitude play a significant role. Here we search for the $b \to sd\overline{d}$ decay $B^0 \to \omega K^{*0}$ (Fig. 1), which has not yet been observed [5, 6]. The expected standard model (SM) rate is small [7], and observing an enhancement above this rate could indicate new physics. Furthermore, $B^0 \to \omega K^{*0}$ decays can be useful for determining the Cabibbo-Kobayashi-Maskawa (CKM) [8] angle $\phi_3(= \gamma)$ [9].

This analysis uses 479 fb^{-1} of data containing 520×10^6

$B\overline{B}$ pairs. The data was collected with the Belle detector [10] at the KEKB [11] e^+e^- asymmetric-energy (3.5 GeV on 8.0 GeV) collider with a center-of-mass (CM) energy at the $\Upsilon(4S)$ resonance. The production rates of $B^0\overline{B}^0$ and B^+B^- pairs are assumed to be equal.

The Belle detector is a large-solid-angle spectrometer. It consists of a silicon vertex detector (SVD), a 50-layer central drift chamber (CDC), an array of aerogel threshold Cherenkov counters (ACC), time-of-flight scintillation counters (TOF), and an electromagnetic calorimeter comprised of CsI(Tl) crystals located inside a superconducting solenoid coil that provides a 1.5 T magnetic field. An iron flux return located outside the coil is instrumented to detect K^0_L mesons and to identify muons (KLM).

The B-daughter candidates are reconstructed through their decays $\omega \to \pi^+\pi^-\pi^0$, $K^{*0} \to K^+\pi^-$ and $\pi^0 \to \gamma\gamma$ [12]. A charged track is identified as a pion or kaon by combining information from the CDC, ACC and TOF systems. We reduce the number of poor quality tracks by requiring that $|dz| < 4.0$ cm and $dr < 0.2$ cm, where $|dz|$ and dr are the closest approach of a track to the interaction point in the z-direction and in the transverse plane, respectively. In addition, we require that each charged track have a transverse momentum $p_T > 0.1$ GeV/c and a minimum number of SVD hits. Tracks matched with clusters in the ECL that are consistent with an electron hypothesis are rejected.

Candidate π^0 mesons are reconstructed from pairs of photons, where the energy of each photon in the laboratory frame is required to be greater than 100 MeV for the ECL endcap regions ($17^\circ < \theta < 32^\circ$ or $129^\circ < \theta < 150^\circ$) and 50 MeV for the ECL barrel region ($32^\circ < \theta < 129^\circ$), where θ denotes the polar angle with respect to the beam axis. We select π^0 mesons with an invariant mass in the range 0.1178 GeV/$c^2 < M_{\gamma\gamma} < 0.1502$ GeV/c^2 and a momentum in the laboratory frame $p_{\pi^0} > 0.39$ GeV/c.

We define ω and K^{*0} signal regions 0.73 GeV/$c^2 < M_{\pi\pi\pi} < 0.83$ GeV/c^2 and 0.755 GeV/$c^2 < M_{K\pi} < 1.050$ GeV/c^2, respectively. In the maximum-likelihood (ML) fit described below, the K^{*0} fit region extends to 0.755 GeV/$c^2 < M_{K\pi} < 1.250$ GeV/c^2 to allow for greater discrimination between signal $B^0 \to \omega K^{*0}$ and non-resonant $B^0 \to \omega K^+\pi^-$ decays. To reduce combinatorial background arising from low-momentum kaons and pions, we require that $\cos\theta_{K\pi} > -0.8$, where $\theta_{K\pi}$ is the angle between the direction of the K^+ and the direction opposite to the B^0 momentum in the K^{*0} rest frame.

Candidate $B^0 \to \omega K^{*0}$ decays are identified using the energy difference (ΔE) and the beam-energy-constrained mass ($M_{\rm bc}$). They are defined as $\Delta E \equiv E_B - E_{\rm beam}$ and $M_{\rm bc} \equiv \sqrt{E^2_{\rm beam} - p^2_B}$, where $E_{\rm beam}$ denotes the beam energy and E_B and p_B denote the energy and momentum, respectively, of the candidate B-meson, all evaluated in the e^+e^- CM frame. We select events satisfying $|\Delta E| < 0.2$ GeV and 5.20 GeV/$c^2 < M_{\rm bc} < 5.29$ GeV/c^2, and define signal regions -0.10 GeV $< \Delta E < 0.06$ GeV and 5.27 GeV/$c^2 < M_{\rm bc} < 5.29$ GeV/c^2.

The dominant source of background arises from random combinations of particles in continuum $e^+e^- \to q\overline{q}$ events ($q = u, d, s, c$). To discriminate spherical-like $B\overline{B}$ events from jet-like $q\overline{q}$ events, we use event-shape variables, specifically, 16 modified Fox-Wolfram moments combined into a Fisher discriminant, $\mathcal{F}$ [13]. Additional discrimination is provided by θ_B, the polar angle in the CM frame between the B direction and the negative direction of the positron beam axis. True B mesons follow a $1-\cos^2\theta_B$ distribution, while candidates in the continuum are approximately uniformly distributed in $\cos\theta_B$. The displacement along the beam axis between the signal B vertex and that of the other B, Δz, is also used. This variable provides discrimination against continuum events, whose tracks typically have a common vertex.

Further discrimination against continuum background is achieved through the use of b-flavor tagging information. The flavor of the B meson accompanying the signal candidate is identified via its decay products: charged leptons, kaons, and Λ's. The Belle tagging algorithm [14] yields the flavor of the tagged meson, q $(= \pm 1)$, and a flavor-tagging quality factor, r. The latter ranges from zero for no flavor discrimination to one for unambiguous flavor assignment. For signal events, q is usually consistent with the flavor opposite to that of the signal B, while it is random for continuum events. Thus, the quantity qrF_B is used to separate signal and continuum events, where F_B is the flavor of the signal B as indicated by the charge of the final state kaon: $F_B = +1(-1)$ for B^0 ($\overline{B}^0$).

We use Monte Carlo (MC) simulated signal [15] and data sideband events (defined as 5.20 GeV/$c^2 < M_{\rm bc} <$ 5.26 GeV/c^2, $|\Delta E| < 0.2$ GeV) to form $\mathcal{F}$ and obtain the $\cos\theta_B$, Δz and qrF_B distributions. Our signal MC is generated to be 50% longitudinally polarized ($f_L = 0.5$). Probability density functions (PDFs) derived from $\mathcal{F}$, the $\cos\theta_B$ distributions, and the Δz distributions are multiplied to form signal ($\mathcal{L}_S$) and continuum background ($\mathcal{L}_{q\overline{q}}$) likelihood functions. These are combined to form a likelihood ratio $\mathcal{R} = \mathcal{L}_S/(\mathcal{L}_S + \mathcal{L}_{q\overline{q}})$. We divide the events into six bins of qrF_B and determine the optimum $\mathcal{R}$ selection criteria for each bin by maximizing

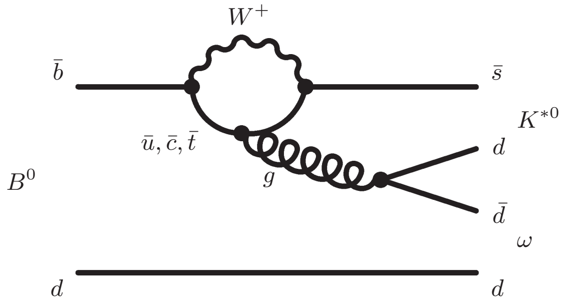

FIG. 1: Penguin diagram for $B^0 \to \omega K^{*0}$ decays.

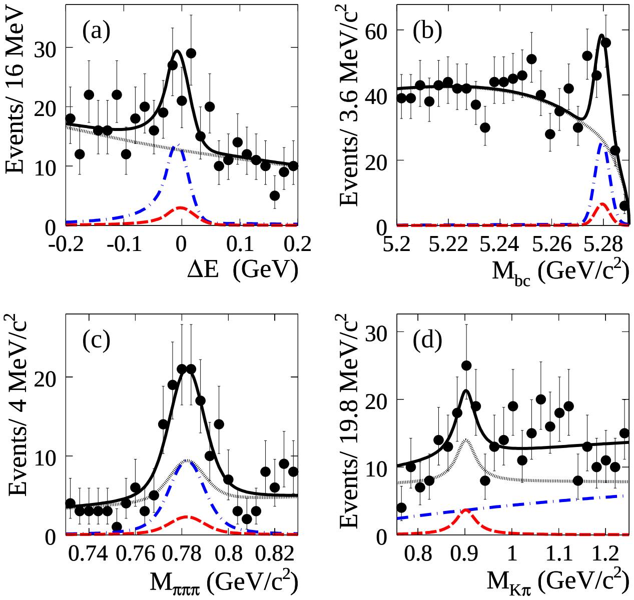

FIG. 2: Projections of ΔE (a), $M_{\rm bc}$ (b), $M_{\pi\pi\pi}$ (c) and $M_{K\pi}$ (d) for events in the signal region of the other three variables. The solid curve is the fit function, the dashed curve is the $B^0 \to \omega K^{*0}$ component, the dot-dashed curve is the $B^0 \to \omega K^+\pi^-$ component, and the dotted curve is the sum of the $q\overline{q}$, $b \to c$ and $b \to s,u,d$ components.

$\mathcal{N}_S/\sqrt{\mathcal{N}_S + \mathcal{N}_{BG}}$, where $\mathcal{N}_S$ is the number of signal MC events in the signal region, and $\mathcal{N}_{BG}$ is the number of background events estimated to be in the signal region by extrapolating from the data sideband. This optimization preserves 50% of the signal while rejecting 99% of the continuum background.

After all selection requirements, 12% of events in the signal MC have more than one candidate. We choose the best candidate in an event to be the one that minimizes the quantity $|M_{\gamma\gamma} - M_{\pi^0}|$. From MC simulation, we find that 8.5% of signal decays have at least one particle incorrectly identified but pass all selection criteria. We refer to these as "self-cross-feed" (SCF) events. The remaining signal events, from correctly reconstructed $B^0 \to \omega K^{*0}$ decays, are referred to as "true-signal" decays.

We obtain the signal yield using a four-dimensional extended unbinned ML fit to ΔE, $M_{\rm bc}$, $M_{\pi\pi\pi}$ and $M_{K\pi}$. The likelihood function consists of the following components: true-signal decays, SCF events, non-resonant $\omega K\pi$ decays, continuum background ($q\overline{q}$), charm B-decay background ($b \to c$), and charmless B-decay background ($b \to s,u,d$). For all components, no sizable correlations are found among the fitted quantities. The PDF for event i and component j is defined as

$$\mathcal{P}_j^i = \mathcal{P}_j(\Delta E^i)\mathcal{P}_j(M_{\rm bc}^i)\mathcal{P}_j(M_{\pi\pi\pi}^i)\mathcal{P}_j(M_{K\pi}^i). \quad (1)$$

For the true-signal, non-resonant, and peaking components of the $q\overline{q}$ and $b \to s,u,d$ backgrounds, the K^{*0} and ω resonances are modeled with Breit-Wigner functions whose widths are fixed to their PDG [16] values. The Breit-Wigner used to describe the ω resonance is convolved with a Gaussian of $\sigma = 5.7$ MeV to account for the detector resolution. This value, along with the means for both resonances and the fraction of peaking $q\overline{q}$ background events, are obtained from one-dimensional fits to $M_{K\pi}$ and $M_{\pi\pi\pi}$ for events in the data sideband region.

All other parameters are obtained from MC simulation. For the true-signal and non-resonant components, the sum of a Crystal Ball line shape (CBLS) [17] and Gaussian with a common mean is used to describe ΔE, and the sum of two Gaussians with a common mean is used to describe $M_{\rm bc}$. To take into account small differences between the MC and data, the $M_{\rm bc}$- ΔE shapes for the true-signal and non-resonant PDFs are corrected according to calibration factors determined from large $B^0 \to D^-\rho^+$, $D^- \to K^+\pi^-\pi^-$ control samples in data and MC. To describe the non-resonant $M_{K\pi}$ component, we use a second-order Chebyshev polynomial. The SCF events are modeled with non-parametric PDFs using Kernel Estimation [18].

The $M_{\rm bc}$ PDF for $q\overline{q}$ background is modeled by a threshold ARGUS [19] function. A first-order Chebyshev polynomial is used to model ΔE and the combinatorial components of $M_{\pi\pi\pi}$ and $M_{K\pi}$. The PDF for $b \to c$ is the product of an ARGUS function for $M_{\rm bc}$, and second-order Chebyshev polynomials for ΔE, $M_{K\pi}$ and $M_{\pi\pi\pi}$. To model the $b \to s,u,d$ background we use a fifth-order Chebyshev polynomial for ΔE and a Gaussian plus ARGUS function for $M_{\rm bc}$. For the non-peaking component of $M_{\pi\pi\pi}$ and $M_{K\pi}$ we use first- and second-order Chebyshev polynomials, respectively.

The following parameters are allowed to vary in our final fit to the data: the true-signal, non-resonant, $b \to c$ and $q\overline{q}$ yields, and the $q\overline{q}$ PDF parameters describing the ΔE, $M_{\rm bc}$ and combinatorial shapes of $M_{\pi\pi\pi}$ and $M_{K\pi}$. The fraction of SCF events is fixed to be 8.5% of the signal. The fraction of $b \to s,u,d$ events is very small (0.7%) and thus is also fixed in the fit according to the predictions of MC simulation.

The likelihood function for event i is given by

$$\mathcal{L} = \frac{e^{-(\sum Y_j)}}{N!}\prod_{i=1}^{N}\sum_j Y_j \mathcal{P}_j^i, \quad (2)$$

where Y_j is the yield of events from component j and N is the total number of events in the sample.

The results of the fit are shown in Fig. 2. We find strong peaking in ΔE, $M_{\rm bc}$ and $M_{\pi\pi\pi}$, which have shapes consistent with those observed in MC simulations. However, we do not observe a strong K^{*0} resonance. Instead, we observe a high density of events in the upper sideband of the $M_{K\pi}$ distribution, which the fit assigns to non-resonant decays. The branching fraction is evalu-

TABLE I: Systematic errors for $\mathcal{B}(B^0 \to \omega K^{*0})$.

Type	Fractional error (%)	
	$+\sigma$	$-\sigma$
Track reconstruction efficiency	4.80	-4.80
π^0 reconstruction efficiency	4.00	-4.00
$K^\pm\pi^\pm$ idenfication efficiency	1.33	-1.33
ΔE PDF shape calibration	3.46	-3.62
$M_{\rm bc}$ PDF shape calibration	2.12	-2.19
Shape of K^{*0} and ω PDFs	3.45	-3.69
Shape of true-signal PDF	0.69	-0.69
Shape of $B^0 \to \omega K^+\pi^-$ PDF	9.02	-5.80
Shape of $b \to c$ PDF	1.50	-1.60
Shape of $b \to s, u, d$ PDF	1.02	-1.09
Shape of $q\overline{q}$ PDF	6.65	-6.16
Fraction of $b \to s, u, d$ background	2.59	-5.04
SCF fraction	5.66	-5.17
Possible fitting bias	1.50	0.00
Effect of higher K^{*0} resonances	1.30	0.00
$B^0 \to \omega K^{*0}$ acceptance	0.63	-0.63
Longitudinal polarization	2.61	-2.61
$\mathcal{R}$ requirement	2.80	-2.80
$N_{B\bar{B}}$	1.31	-1.31
Total	**16.1**	**-14.7**

ated using the following quantities: $Y_{\omega K^{*0}} = 15.1^{+11.1}_{-10.0}$, the signal yield; $\varepsilon = (4.48 \pm 0.03) \times 10^{-2}$, the signal efficiency; $\varepsilon_{\rm track} = 0.94 \pm 0.01$, an efficiency correction for the charged track selection that takes into account small differences between MC and data; $(520 \pm 6) \times 10^6$, the number of $B\overline{B}$ pairs produced; and $\prod \mathcal{B}_i = 0.59 \pm 0.01$ ($i = K^{*0}, \omega, \pi^0$), the product of daughter branching fractions.

The sources of systematic error are listed in Table I. The errors on the PDF shapes are obtained by varying all fixed parameters by $\pm 1\sigma$. To obtain the error on the SCF and $b \to s, u, d$ fractions, we vary the normalizations by $\pm 50\%$. The effect of a possible fit bias due to floating the non-resonant $\omega K\pi$ normalization is obtained by fitting ensembles of simulated experiments containing varying sets of signal and non-resonant events. We consider the effects of higher K^{*0} resonances by calculating the fractional change in our signal yield when we include a PDF for $B^0 \to \omega K^{*0}(1430)$, whose yield is fixed to 1.0 event, as determined by extrapolating from a higher-mass region. The dependance of the acceptance on f_L is obtained by varying f_L from 0 to 1.0. To obtain the uncertainty on the selection efficiency of the $\mathcal{R}$ requirement, we vary the $\mathcal{R}$ thresholds, and we also calculate the data/MC efficiency ratio for the $B^0 \to D^-\rho^+$, $D^- \to K^+\pi^-\pi^-$ control sample.

Our final result for the branching fraction based on 520×10^6 $B\overline{B}$ pairs is

$$\mathcal{B}(B^0 \to \omega K^{*0}) = [1.2^{+0.9}_{-0.8} \pm 0.2\ (< 2.7)] \times 10^{-6}, \quad (3)$$

where the first error quoted is statistical, the second systematic, and the upper limit is taken to be the branching fraction corresponding to 90% of the total integral of the likelihood function in the positive branching fraction region. The systematic error is included by convolving the likelihood function with a Gaussian having a standard deviation equal to the systematic uncertainty. The statistical significance of the signal, defined as $\sqrt{-2\ln(\mathcal{L}_0/\mathcal{L}_{\rm max})}$, where $\mathcal{L}_{\rm max}$ ($\mathcal{L}_0$) is the value of the likelihood function when $Y_{\omega K^{*0}}$ is allowed to vary (set to 0), is 1.6σ.

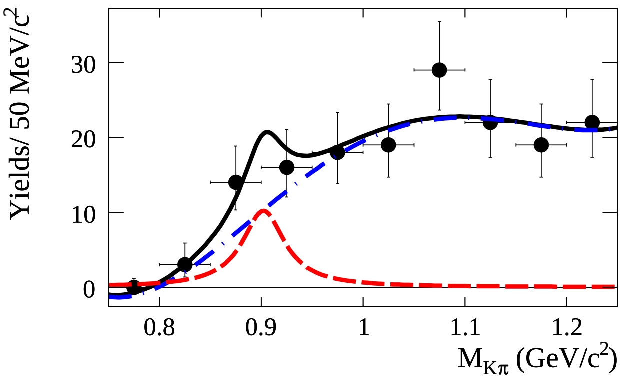

FIG. 3: Signal yields obtained from the ΔE-$M_{\rm bc}$ distribution in bins of $M_{K\pi}$ for events in the ω signal region. The solid curve is the fit function, the dashed curve is the $B^0 \to \omega K^{*0}$ component, and the dot-dashed curve is the $B^0 \to \omega K^+\pi^-$ component.

To verify the large non-resonant contribution, we fit the background-subtracted $M_{K\pi}$ distribution to extract the signal yield. To obtain this distribution, we bin the data in $M_{K\pi}$ from [0.75, 1.25] GeV/c^2 and, for each bin, perform a two-dimensional extended unbinned ML fit to ΔE and $M_{\rm bc}$. The likelihood function consists of three components: signal + non-resonant, $q\overline{q} + b \to c$, and $b \to s, u, d$. We use a single PDF to describe the signal + non-resonant component, since their individual shapes are almost identical in ΔE and $M_{\rm bc}$. A single PDF is also used to model $q\overline{q} + b \to c$, since in several of the bins, the statistics are too low to model them independently. The ΔE and $M_{\rm bc}$ PDFs for the signal + non-resonant and $b \to s, u, d$ components are identical to those used in the four-dimensional fit, with the exception that here, we do not model the true-signal and SCF events separately. For the $q\overline{q} + b \to c$ PDF, we use a first order Chebyshev polynomial for ΔE and an ARGUS function for $M_{\rm bc}$. We fix the shapes of the signal + non-resonant and $b \to s, u, d$ components from MC simulation. In the final fit, we fix the fraction of $b \to s, u, d$, while allowing the other two normalizations, and the ΔE and $M_{\rm bc}$ shapes of the $q\overline{q} + b \to c$ PDF, to vary.

The results are shown in Fig. 3. We perform a χ^2 fit to this background-subtracted $M_{K\pi}$ distribution. The Breit-Wigner shape is obtained in the same way as for the four-dimensional fit. For the non-resonant component, we use a fourth-order Chebyshev polynomial. In the final fit, we float the non-resonant shape parameters along with the fractional signal yield. We obtain $Y_{\omega K^{*0}}/(Y_{\omega K^{*0}}+Y_{\omega K\pi}) = (9.3\pm10.6)\%$, which is very similar to the result of the four-dimensional fit: $(10.3^{+7.7}_{-7.0})\%$.

In summary, we present a measurement of the branching fraction of $B^0 \to \omega K^{*0}$ decays using 520×10^6 $B\overline{B}$ pairs. The statistical significance of our signal yield is only 1.6σ, and thus we set an upper limit of $\mathcal{B} < 2.7\times10^{-6}$ at the 90% C.L. Our result is in agreement with theoretical estimates [7]. The limit obtained is below the previous constraint from BaBar [6] by a factor of 1.6. In addition, we observe a large rate for non-resonant $B^0 \to \omega K^+\pi^-$ decays.

We thank the KEKB group for the excellent operation of the accelerator, the KEK cryogenics group for the efficient operation of the solenoid, and the KEK computer group and the National Institute of Informatics for valuable computing and Super-SINET network support. We acknowledge support from the Ministry of Education, Culture, Sports, Science, and Technology of Japan and the Japan Society for the Promotion of Science; the Australian Research Council and the Australian Department of Education, Science and Training; the National Science Foundation of China and the Knowledge Innovation Program of the Chinese Academy of Sciences under contract No. 10575109 and IHEP-U-503; the Department of Science and Technology of India; the BK21 program of the Ministry of Education of Korea, the CHEP SRC program and Basic Research program (grant No. R01-2005-000-10089-0) of the Korea Science and Engineering Foundation, and the Pure Basic Research Group program of the Korea Research Foundation; the Polish State Committee for Scientific Research; the Ministry of Education and Science of the Russian Federation and the Russian Federal Agency for Atomic Energy; the Slovenian Research Agency; the Swiss National Science Foundation; the National Science Council and the Ministry of Education of Taiwan; and the U.S. Department of Energy.

[1] Belle Collaboration, Y. Chao *et al.*, Phys. Rev. Lett. **93**, 191802 (2004).

[2] BaBar Collaboration, B. Aubert *et al.*, Phys. Rev. Lett. **93**, 131801 (2004); BaBar Collaboration, B. Aubert *et al.*, hep-ex/0703016. Submitted to Phys. Rev. Lett.

[3] Belle Collaboration, K.F. Chen *et al.*, Phys. Rev. Lett. **91**, 201801 (2003); Belle Collaboration, K.F. Chen *et al.*, Phys. Rev. Lett. **94**, 221804 (2005).

[4] BaBar Collaboration, B. Aubert *et al.*, Phys. Rev. Lett. **91**, 171802 (2003); BaBar Collaboration, B. Aubert *et al.*, Phys. Rev. Lett. **93**, 231804 (2004); BaBar Collaboration, B. Aubert *et al.*, arXiv:0705.1798, submitted to Phys. Rev. Lett.

[5] BaBar Collaboration, B. Aubert *et al.*, Phys. Rev. D **71**, 031103 (2005).

[6] BaBar Collaboration, B. Aubert *et al.*, Phys. Rev. D **74**, 051102 (2006).

[7] G. Kramer and W.F. Palmer, Phys. Rev. D **45**, 193 (1992); G. Kramer and W.F. Palmer, Phys. Rev. D **46**, 2969 (1992); A. Ali, G. Kramer, and C.-D. Lü, Phys. Rev. D **58**, 094009 (1998); A. Ali, G. Kramer, and C.-D. Lü, Phys. Rev. D **59**, 014005 (1999); Y.H. Chen *et al.*, Phys. Rev. D **60**, 094014 (1999); H. Y. Cheng and K.C. Yang, Phys. Lett. B **511**, 40 (2001).

[8] M. Kobayashi and T. Maskawa, Prog. Theor. Phys. 49, 652 (1973); N. Cabibbo, Phys. Rev. Lett. **10**, 531 (1963).

[9] D. Atwood and A. Soni, Phys. Rev. D **59**, 013007 (1999); D. Atwood and A. Soni, Phys. Rev. D **65**, 073018 (2002); H.-W. Huang *et al.*, Phys. Rev. D **73**, 014011 (2006).

[10] Belle Collaboration, A. Abashian *et al.*, Nucl. Instrum. Methods Phys. Res., Sect. A **479**, 117 (2002).

[11] S. Kurokawa and E. Kikutani, Nucl. Instrum. Methods Phys. Res., Sect. A **499**, 1 (2003), and other papers in this volume.

[12] Charge-conjugate decays are included unless explicitly stated otherwise.

[13] The Fox-Wolfram moments were introduced in G. C. Fox and S. Wolfram, Phys. Rev. Lett. **41**, 1581 (1978). The modified moments used in this Letter are described in Belle Collaboration, S. H. Lee *et al.*, Phys. Rev. Lett. **91**, 261801 (2003).

[14] H. Kakuno *et al.*, Nucl. Instrum. Methods Phys. Res., Sect. A **533**, 516 (2004).

[15] Evtgen generator, D. J. Lange, Nucl. Instrum. Methods Phys. Res., Sect. A **462**, 152 (2001). The detector response is simulated with GEANT, R. Brun *et al.*, GEANT 3.21, CERN Report DD/EE/84-1, 1984.

[16] Particle Data Group, S. Eidelman *et al.*, Phys. Lett. B **592**, 1 (2004).

[17] T. Skwarnicki, Ph.D. Thesis, Institute for Nuclear Physics, Krakow 1986; DESY Internal Report, DESY F31-86-02 (1986).

[18] Kernel Estimation in High-Energy Physics, *K. Cranmer*, Comput. Phys. Commun. 136 (2001) 198207, hep-ex/0011057.

[19] ARGUS Collaboration, H. Albrecht *et al.*, Phys. Lett. B **241**, 278 (1990).